Eur. Phys. J. Spec. Top. (2022) 231:3281–3287
https://doi.org/10.1140/epjs/s11734-022-00658-8

THE EUROPEAN PHYSICAL JOURNAL SPECIAL TOPICS

Regular Article

Exploration of stochastic dynamics and complexity in an epidemic system

Shaobo He[1,a] and Sayan Mukherjee[2,b]

[1] School of Physics and Electronics, Central South University, 932, Lushan South Road, Changsha 410083, Hunan, China
[2] Department of Mathematics, Sivanath Sastri College, 23/49, Gariahat Road, Kolkata 700029, West Bengal, India

Received 29 April 2022 / Accepted 5 August 2022 / Published online 29 August 2022
© The Author(s), under exclusive licence to EDP Sciences, Springer-Verlag GmbH Germany, part of Springer Nature 2022

Abstract We investigate the effect of noise in an epidemic system. We have studied dynamics and complexity for both the deterministic and its noise-induced model. We have verified the stochastic sensitivity under the variation of noise strength and changing the initial conditions of the noise-induced system. It confirms that noise can make significant perturbation in the stochastic sensitivity. To quantify the dynamics, phase space analysis is done under both noisy and noise free conditions. The transition between regular and chaotic dynamics has been examined by $0--1$ test. Corresponding complexity analysis is also done using the weighted recurrence entropy method. Numerical results confirm the chaotic dynamics in the noise-induced epidemic system within a larger region of parameters compared to the same in its noise free part.

1 Introduction

Ecosystem is one of the highly nonlinear systems that can be observed in many real word phenomena [1]. A nonlinear system can produces various kind of long-term dynamics [2–7]. Several studies have been done for the ecosystems, that show existence of regular as well as chaotic long-term dynamics [8–15, 27, 28]. The most well-known chaotic illustration can be given by the logistic map-a discrete system of animal reproduction [8]. Chaotic behaviour has been also observed for the continuous ecological system in many literature [9–19, 26]. In [27], it has been proved that chaos is one of the destabilizing factors that can collapse ecosystems. Further, a stabilizing effect of chaos is also observed in [28] that implies re-immigration or rescue effect in the ecosystem. Thus, chaotic dynamics is an obvious property in ecosystems and hence the corresponding future is almost unpredictable [17–19, 26].

Chaos in a nonlinear system is such a state that shows sensitivity with initial condition [3–5]. In that case, the system losses its memory with a small perturbation of the initial condition [3–5]. Chaos can be investigated for both deterministic and stochastic system [3–7, 29–33]. For a deterministic system, Lyapunov analysis is one of the efficient methods for finding chaos in the corresponding system [3–5]. To investigate chaos in a stochastic system, the $0-1$ test method is one of the effective nonlinear tools [34–37].

A chaotic system always has unpredictable behaviour. So uncertainty is a ubiquitous property of this system. For a stochastic phenomenon, it is more than a deterministic phenomenon. It means that the uncertainty increases as the system becomes more and more random. The measure of uncertainty was first introduced by C.E. Shannon [38]. Several entropy measures have been developed and applied widely in diverse domains of research [20–25]. Complexity in a system can be characterized by measuring disorder in the corresponding phase space [39–45]. Different types of measures have been proposed to quantify dynamical complexity of a system [41–48]. A weighted recurrence based measure has been proposed in [48], which can describe the different structural patterns of the phase space. The proposed weighted entropy measure correlates to the dynamics of the system (discrete or continuous) [48].

Noise is an inherent feature that appears in different forms in the real world phenomena. Several research have been established on the effect of noise in different systems [29–33, 45]. Further, the effect of noise in the epidemic has been already established in the literature [16–18]. So, noise-induced long-term analysis is one of the best possible studies to approximate the dynamics of a stochastic epidemic system. In [26], the chaotic phenomenon and its relation with the diseases have been investigated in the context of generalist predators. The effect of noise is not examined for the system given in [26]. We, therefore, studied the impact of noise on an epidemic system using measures of chaos and complexity.

[a] e-mail: heshaobo@csu.edu.cn
[b] e-mail: msayan80@gmail.com (corresponding author)

This article is organized as follows: In section 2, a stochastic epidemic system is constructed. Section 3 described stochastic sensitivity [53] of the noise induced epidemic system. Using $0-1$ test method, dynamical fluctuation is analyzed over the feasible ranges of disease reproduction and noise strength. The whole discussion is given in Sect. 4. Section 5 discusses the complexity of the phase spaces based on weighted recurrence entropy analysis. Finally, a conclusion is given in Sect. 6.

2 Construction of stochastic epidemic model

We consider an epidemic model, proposed in [26], given by

$$\begin{aligned}\frac{dx_1}{dt} &= ax_1 - Rx_1x_2 - ax_1x_4,\\ \frac{dx_2}{dt} &= Rx_1x_2 - ax_2x_4 - x_2,\\ \frac{dx_3}{dt} &= bx_3 - acx_3x_4,\\ \frac{dx_4}{dt} &= d(x_1+x_2+x_3)x_4 - dx_4,\end{aligned} \tag{1}$$

where x_1, x_2 are healthy and infected variables of the susceptible species respectively. The variable x_3 represents population of the immune prey species. The last variable x_4 indicates predator population of the system. The parameters a, b represent the reproduction rate of the prey species. R denotes the basic reproduction number of the disease. The parameters c and d is defined in [26] by $c = \frac{\epsilon_y}{\epsilon_x}$ ($\epsilon_{x,y}$ are rates of individual prey species) and $d = \frac{\delta}{\gamma}$ (δ, γ are the predator starvation rate in the absence of prey and death rate of infected individual prey species respectively). A complete pictorial representation of the system (1) is given in Fig. 1.

To construct the stochastic version of (1), we incorporate noise $\Phi(\alpha)$ for the healthy population rate. The noise $\Phi(\alpha)$ is taken as $\frac{1}{f}$noise. Incorporation of noise in the deterministic system and its converted system is shown in Fig. 1. The reason for inducing the $\frac{1}{f}$-noise can be stated as follows: (i) $\frac{1}{f}$-noise has long-range dependence [49–52]. It affects the long-term dynamics of the system, ii) fluctuation of $\frac{1}{f}$-noise can be observe in many physical phenomena [49–52]. As the dynamics of an epidemic depend on the interaction of prey and predator populations, the effect of $\frac{1}{f}$-noise is an obvious phenomenon in the epidemic system. The constructed noise-induced epidemic model is then given by

$$\begin{aligned}\frac{dx_1}{dt} &= ax_1 - Rx_1x_2 - ax_1x_4 + K\Phi(\alpha),\\ \frac{dx_2}{dt} &= Rx_1x_2 - ax_2x_4 - x_2,\\ \frac{dx_3}{dt} &= bx_3 - acx_3x_4,\\ \frac{dx_4}{dt} &= d(x_1+x_2+x_3)x_4 - dx_4,\end{aligned} \tag{2}$$

where function $\Phi(\alpha)$ represents $\frac{1}{f}$ power noise and K its strength respectively. We fix $a = \frac{7}{400}, b = 0.0208, c = 1.5, d = 0.3098$ as taken in [26]. We only variate R, K by $R \in [1, 1.5]$ and $K \in [0, 0.5]$ respectively.

In the following section, we investigate stochastic sensitivity of the system (2) under the variation of noise strength (K) and initial condition.

3 Stochastic sensitivity

To quantify stochastic sensitivity, we consider $4D$ attractors of the system (2) with the initial condition $(x_1(0), x_2(0), x_3(0), x_4(0)) = (1, 0.2, 0.4, 0.1)$. As this system possesses an equilibrium state for $a = 7/400, b = 0.0208, c = 1.5, d = 0.3098, R = 1.0205$ [26], we consider (1, 0.2, 0.4, 0.1) as an equilibrium point and call it $\bar{x}$. According to the definition of quasipotential [53], the function $v(x)$ of the $4D$ attractors is given by

$$v(x) \approx \frac{1}{2}(x - \bar{x}, \phi(x)(x - \bar{x})),$$

where $x = (x_1(t), x_2(t), x_3(t), x_4(t))$. It can be approximated by Gaussian density function $\rho(x, K)$ of the random trajectory flow in the attractors, where

$$\rho(x, K) \approx Nexp(-\frac{(x - \bar{x}, W^{-1}(x - \bar{x}))}{2K^2}),$$

where $W = \phi^{-1}(\bar{x})$ and N being a normalized constant [53].

The density function $\rho(x, K)$ of the random state in the neighbourhood of $\bar{x}$ can be geometrically described by a confidence ellipsoid [53]. The confidence ellipsoid is defined as

$$(x - \bar{x}, W^{-1}(x - \bar{x})) = K^2\Gamma(P),$$

where P represents fiducial probability. Here, $\Gamma(P)$ is an inverse of $P(\Gamma)$ which is defined by

$$P(\Gamma) = \frac{\phi_n(\Gamma)}{\phi_n(\infty)}, \phi_n(\Gamma) = \int_0^{\sqrt{\Gamma}} e^{-\frac{t^2}{2}} t^{n-1} dt.$$

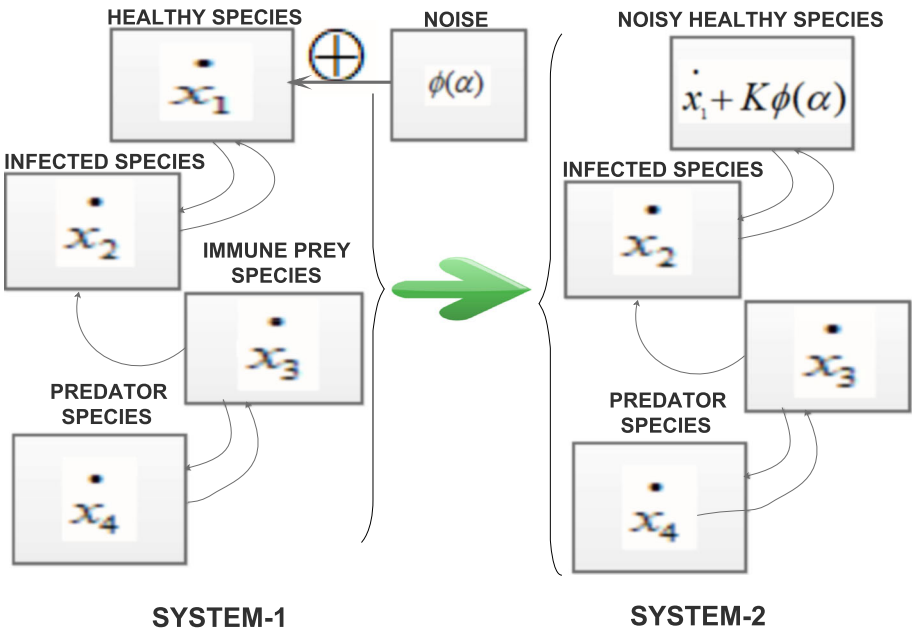

Fig. 1 Representing the conversion of deterministic (SYSTEM-1) to noise-induced (SYSTEM-2) epidemic system. Green arrow indicates the conversion from SYSTEM-1 to SYSTEM-2. Left arrow with $\oplus$ sign indicates the induction of noise $\phi(\alpha)$ to the healthy population rate $\dot{x}_1$. The corresponding noise affected growth is given by $\dot{x}_1 + K\phi(\alpha)$. The SYSTEM-1 and SYSTEM-2 are given by (1) and (2) respectively. The curved arrows associated with the species are indicated intermediate relations

For $n = 4$, $P(\Gamma)$ is given by $P(\Gamma) = 1 - e^{\frac{\Gamma}{2}}(1 + 0.5\Gamma)$ and the corresponding $4D$ confidence ellipsoid is defined as

$$\frac{\xi_1^2}{\lambda_1} + \frac{\xi_2^2}{\lambda_2} + \frac{\xi_3^2}{\lambda_3} + \frac{\xi_4^2}{\lambda_4} = K^2\Gamma(P), \tag{3}$$

where $\xi_j = (x - \bar{x}, \nu_j)$; $j = 1, 2, 3, 4$ (ν_i being eigenvector for the eigenvalues λ_j; $j = 1, 2, 3, 4$ of the stochastic sensitivity matrix W). As λ_js measure stochastic sensitivity of a system, $\max_{j=1,2,3,4} \lambda_j$ is also effective for the same. We call $\max_{j=1,2,3,4}\{\lambda_j\}$ as Λ_{max} and calculate its fluctuation over $K \in [0.001, 0.1]$ ($R = 1.0205$) and $I_i \in [(1 + 0.0002 * i, 0.2, 0.4, 0.1)]$ ($R = 1.0205$, $K = 0.005$). The corresponding oscillations are shown in Fig. 2a and b respectively. From Fig. 2a, it can be observed that Λ_{max} has nonlinear increasing trend for $K \in [0.001, 0.1]$ ($R = 1.0205$). It indicates sensitivity of (2) increases nonlinearly with the increasing noise strength. On the other hand, a sharp increasing trend in Λ_{max} can be observed in Fig.2b for $I_i \in [(1 + 0.0002 * i, 0.2, 0.4, 0.1)]$ with $R = 1.0205$, $K = 0.005$. It implies increasing stochastic sensitivity in (2) for a small perturbation of $\bar{x}$. Further, oscillations in Λ_{max} are calculated over $(K, I_i) \in [0.001, 0.1] \times [(1 + 0.0002 * i, 0.2, 0.4, 0.1)]$. The corresponding contour plot is visualized in Fig. 2c. From the figure, it can be seen that the Λ_{max} is increasing according to increase of noise strength K within a small neighourhood of $\bar{x}$. So, this analysis indicates effectiveness of power noise on increasing the stochastic sensitivity in the system (2).

We now investigate the dynamics of the system (2) under the variation of basic reproduction number (R) of the disease and noise strength (K).

4 Quantifying dynamics of the noise free and noisy epidemic model

To quantify the dynamics, we first characterize the asymptotic dynamics of (2) using phase space analysis. The phase space analysis is done under the variation of both $R \in [1, 1.5]$ and $K \in [0, 0.5]$ respectively. Some of the phase spaces are projected in $2D$ (see the Fig. 3). From Fig. 3a, periodic orbit can be observed. It indicates regular asymptotic dynamics of the system at ($K = 0$, $R = 0$). On the other hand, irratic movement in phase trajectory can be observed in 3b-d. It indicates complex asymptotic dynamics of the same system with the respective cases $(K = 0.2,\ R = 0), (K = 0,\ R = 1.15), (K = 0.5,\ R = 1.5)$. In this way, we have examined nature of long-term dynamics of (2) for $R \in [1, 1.5]$ and $K \in [0, 0.5]$. However, chaos cannot be confirmed from these phase space analysis. To characterized regular and chaotic dynamics, we have implemented $0 - 1$ chaos test method.

In this method, a solution $\{x(k)\}_{k=1}^{L}$ (L being the length of the solution) is considered of a system. Then, $\{x(k)\}_{k=1}^{N}$ is decomposed into two components p_μ, q_μ, where

$$p_\mu(n) = \sum_{k=1}^{n} x(k)\cos(k\mu), \quad q_\mu(n) = \sum_{k=1}^{n} x(k)\sin(k\mu). \tag{4}$$

In (4), the value of μ can be chosen from the interval $(0, \pi)$ for each n $(= 1, 2, .., L)$. The cloud consists of (p_μ, q_μ) can be characterized by two types of geometric-regular and Brownian motion like structures [34–37].

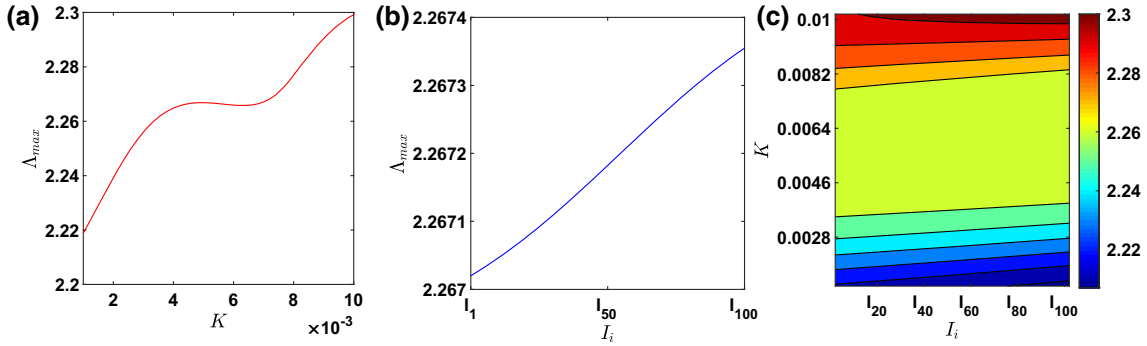

Fig. 2 **a** and **b** represents Λ_{max} vs. K and I_i plots respectively. Variation in Λ_{max} with $K \times I_i$ are given in **c**. The associate colour bar indicates values of Λ_{max}

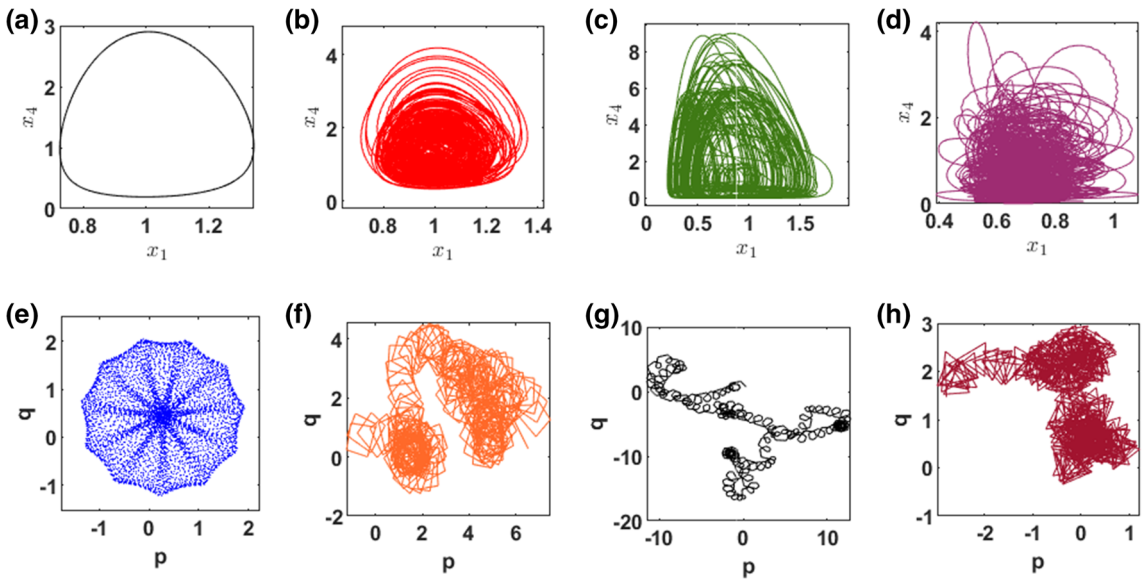

Fig. 3 (a)–(d) represent 2D phase space of the system (2) with $(K = 0,\ R = 0), (K = 0.2,\ R = 0), (K = 0,\ R = 1.15), (K = 0.5,\ R = 1.5)$. Corresponding $(p,\ q)$ plots are given in (e)-(f) respectively. To calculate p and q, we have considered x_1 solution component of (2)

The regular and Brownian motion like structures indicates non-chaotic and chaotic signature in the system respectively [34–37]. The cloud of (p_μ, q_μ) is known as $(p,\ q)$-plot.

We investigate $(p,\ q)$-plots for the system (2) for $R \in [1, 1.5]$ and $K \in [0, 0.5]$. Some of the plots are shown in Fig. 3e-h at $(K = 0,\ R = 0), (K = 0.2,\ R = 0), (K = 0,\ R = 1.15), (K = 0.5,\ R = 1.5)$ respectively.

From the figures, it can be observed that the deterministic structure can only be found in Fig. 3e. The remaining $(p,\ q)$-plots shows always Brownian motion like geometry. So, Fig. 3e indicates non-chaotic dynamics at $(K = 0,\ R = 0)$ and Fig. 3f-h indicate chaos in (2) with $(K = 0.2,\ R = 0), (K = 0,\ R = 1.15), (K = 0.5,\ R = 1.5)$ respectively. Further, chaos is quantified for both the system (1)and (2) with $R \in [1, 1.5]$ (fixed K) and $K \in [0, 0.5]$ (fixed R) respectively.

To quantify chaos, we have implemented a measure τ_μ (Based on p_c, q_c) proposed by Gottwald et.al [35], which can quantifies chaotic as well as non-chaotic dynamics of a system, where

$$\tau_\mu = \lim_{n\to\infty} \frac{\log MD_\mu(n)}{\log n}. \tag{5}$$

Here, $MD_\mu(n)$ is called mean square displacement of the components p_μ, q_μ, given by

$$MD_\mu(n) = \lim_{N\to\infty} \frac{1}{N} \sum_{k=1}^{L} [p_\mu(k+n) - p_\mu(k)]^2 + [q_\mu(k+n) - q_\mu(k)]^2. \tag{6}$$

Figure 4a shows fluctuation of τ_μ over $R \in [1, 1.5]$ with $K = 0$ (blue) and $K = 0.2$ (red) respectively. It can be observed from the figure that, $\tau_\mu < 1$ and ≈ 1 over the respective $R \in [1, 1.14]$ and $R \in (1.14, 1.5]$. However, $\tau_\mu \approx 1$ for all $R \in [1, 1.5]$ can also be observed in the same figure. It indicates chaotic paradigm of

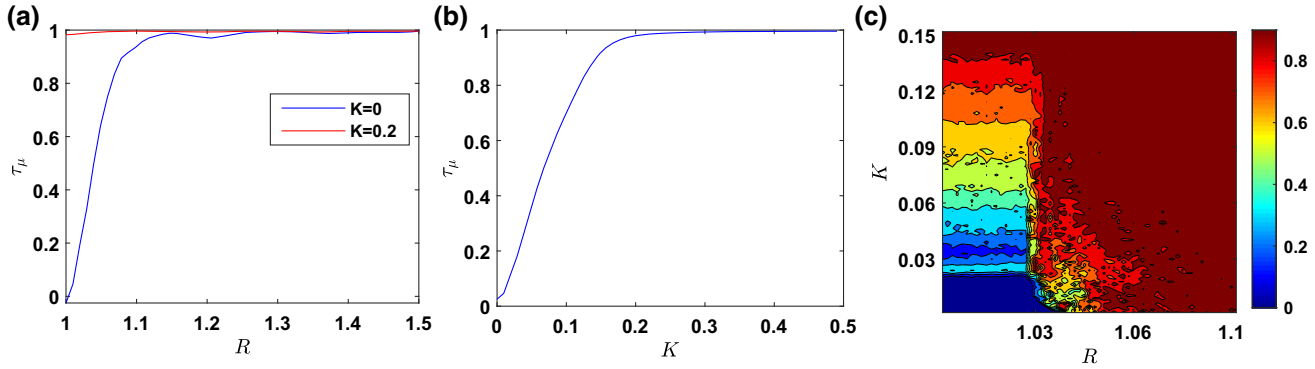

Fig. 4 **a** Represents τ_μ vs. $R(\in [1, 1.5])$ curves with $K = 0$ (blue) and $K = 0.2$ (red) respectively. **b** Represents τ_μ vs. K oscillation with $R = 1.01$. $\tau_\mu(K, R)$-matrix plot is given in **c** with $(K, R) \in [0, 0.15] \times [1, 1.1]$. The coloured bar indicates values of $\tau_\mu(K, R)$

the system (2) increases over $R \in [1, 1.5]$ compare to the same of (1). On the other hand, Fig. 4b indicates that the system can have stochastic chaos for noise strength $K \in [0.15, 5]$ with the fixed $R = 1.01$. From both the observations, it can therefore assure that the noise can enhance complexity in the system (1). Further, oscillation in τ_μ over $(K, R) \in [0, 0.5] \times [1, 1.5]$ is investigated. We only show the oscillation for $(K, R) \in [0, 0.15] \times [1, 1.1]$. The corresponding contour plot is given in Fig. 4c. From the figure, it can be investigated that system (1) can produced chaos for most of the region $(K, R) \in [0, 0.5] \times [1, 1.5]$. It can also verified that the same system shows chaotic phenomena for the region $[0, 0.5] \times [1, 1.5] - [0, 0.15] \times [1, 1.1]$. So, the entire analysis confirms existence of larger chaotic paradigm can be obtained for the system (2) compare to same in (1).

To investigate complexity of the system, we have applied recurrence weight based entropy method [48]. The following section discusses on finding complexity in (1) with noise free and noisy conditions.

5 Quantifying complexity of the noise free and noisy epidemic model

Weighted recurrence (WR) is first developed by Eroglu et al, based on finite dimensional phase space of a nonlinear system [48]. For an n-dimensional phase space $P = \{x_i \in R^n\}$ $(i, j = 1, 2, .., N)$ (N being the length of the trajectory of the phase space), WR is denoted by ω_{ij} and defined as

$$\omega_{ij} = e^{-d_{ij}}. \tag{7}$$

Here, d_{ij} represents distance between two points $x_i, x_j \in R^n$ and it is calculated by $d_{ij} = \|x_i - x_j\|$. As d_{ij} quantifies dispersion between the trajectories, disorder in the phase space can be characterized by $[\omega_{ij}]$-matrix plot. However, values of ω_{ij} are always lies between 0 and 1 as it is defined as exponential decay of d_{ij}. We observed nature of $[\omega_{ij}]$-matrix plots with the variation of $R \in [1, 1.5]$ and $K \in [0, 0.5]$. Figure 5a-d represents some of the $[\omega_{ij}]$-matrix plots of the system (2) with $(K = 0,\ R = 0), (K = 0.25,\ R = 0), (K = 0,\ R = 1.15), (K = 0.5,\ R = 1.5)$. From Fig. 5a, it can be observed that there exists only two variation in the $[\omega_{ij}]$-matrix. It indicates almost homogenous trajectory's pattern in the corresponding phase space. On the other hand, various patterns for the ω_{ij} can be investigated in Fig. 5b–d. It signifies heterogeneous movements in the respective phase trajectory. In this way, we have characterized disorder in the system dynamics for $R \in [1, 1.5]$ and $K \in [0, 0.5]$. Similarly, probability distribution is further investigated by constructing sample space $M = \{\xi : \xi = \frac{1}{N}\sum_{j=1}^{T} \omega_{ij}\}$ (T being number of events). For $(K = 0,\ R = 0), (K = 0.25,\ R = 0), (K = 0,\ R = 1.15), (K = 0.5,\ R = 1.5)$, the corresponding (ξ) vs. ξ curves are shown in Fig. 5e-f respectively. From the figures, it can be seen that only two peaks are exist in Fig. 5e. It indicates only two variation in ξ and hence no disorder in the corresponding phase space. However, large number of peaks can be observed in all the remaining figures (see Fig. 5f-h). It signifies highly disordered phase spaces for the system (2) with $(K = 0.25,\ R = 0), (K = 0,\ R = 1.15), (K = 0.5,\ R = 1.5)$. So, results of probability distribution correlates with the nature of respective $[\omega_{ij}]$-matrix plots as well as system dynamics.

Hence, disorder in the system (2) can be characterized using weighted recurrence.

To quantify the disorder, we used weight recurrence entropy (S) given by

$$S = -\sum_{\xi \in M} p \log p, \tag{8}$$

where $p \equiv p(\xi)$ calculated between $\xi + d\xi$ ($d\xi$ being the small perturbation in ξ).

Figure 6a shows fluctuation in S over $R \in [1, 1.5]$ with $K = 0$ (blue) and $K = 0.2$ (red) respectively. It can be observed from the figure that, $S \in [0.5, 2.9]$ is increasing with $R \in [1, 1.14]$ $(K = 0)$. It indicates

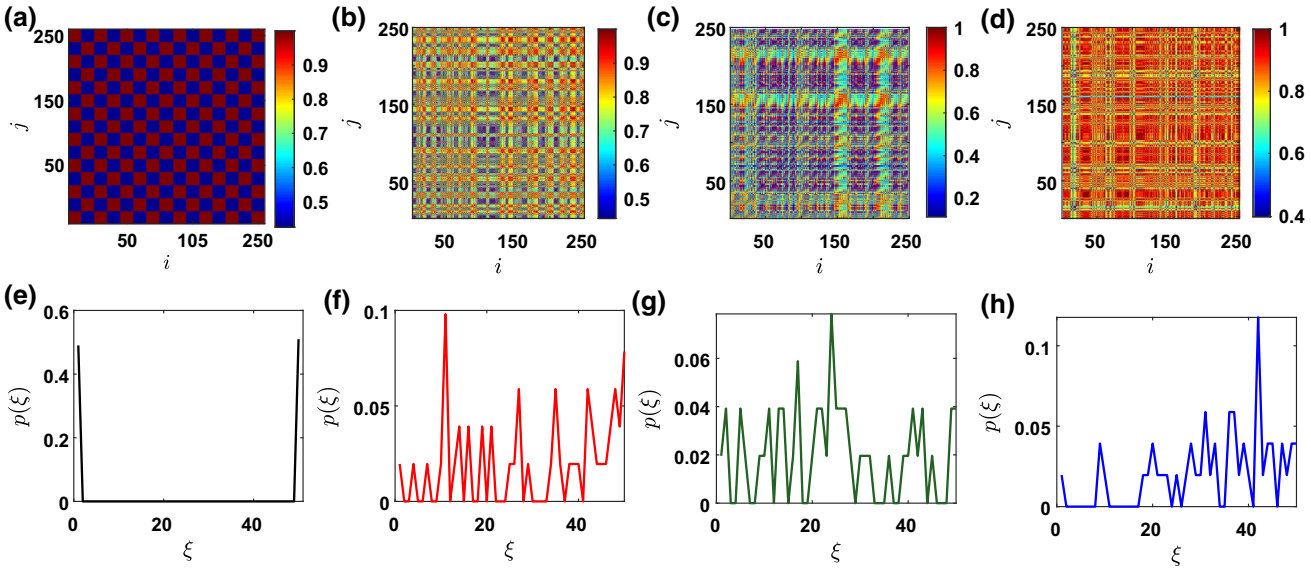

Fig. 5 **a** Weighted recurrence plots for the system (2) with $(K = 0,\ R = 0), (K = 0.25,\ R = 0), (K = 0,\ R = 1.15), (K = 0.5,\ R = 1.5)$ respectively. The corresponding probability density curves are shown in **b**. To count probability $p(\xi)$, we have considered 50 bins

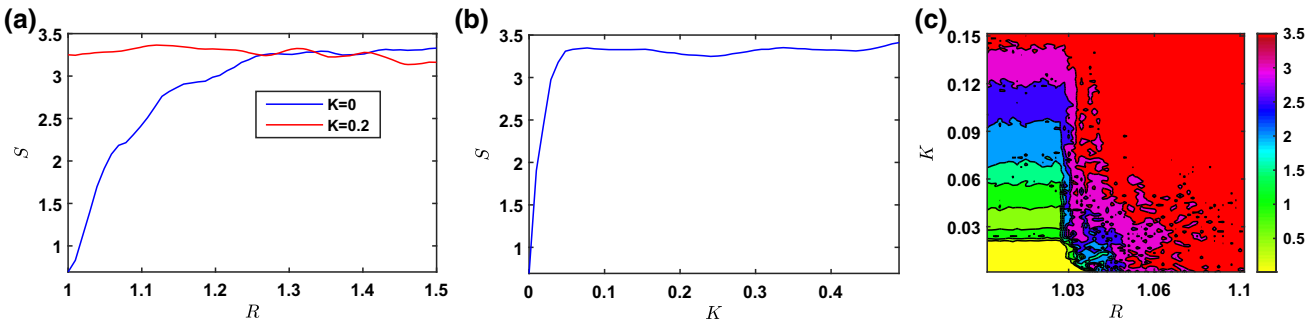

Fig. 6 **a** Represents S vs. $R(\in [1, 1.5])$ curves with $K = 0$ (blue) and $K = 0.2$ (red) respectively. **b** Represents S vs. K oscillation with $R = 1.01$. $S(K,\ R)$-matrix plot is given in **c** with $(K, R) \in [0, 0.15] \times [1, 1.1]$. The coloured bar indicates values of $S(K,\ R)$

that the complexity of the non chaotic dynamics is lies between 0.5 and 2.8. It can be also observed that $S > 3$ with $R \in (1.14, 1.5]$ $(K = 0)$. Further, oscillation in S is always greater than 3 can be seen in the same figure. On the other hand, Fig. 6b indicates that the system produces complexity greater than 3 for $K \in [0.15, 5]$ with the fixed $R = 1.01$. Both the phenomena, strongly correlates with the dynamical fluctuations shown in Fig. 5a and b. In the next, we compute oscillation in S over $(K, R) \in [0, 0.5] \times [1, 1.5]$. Fig. 6c shows fluctuation in S only for $(K, R) \in [0, 0.15] \times [1, 1.1]$. From the figure, it can be investigated that the system (1) reveals phase spaces with $S > 3$ for most of the region $(K, R) \in [0, 0.15] \times [1, 1.1]$. The region of $S > 3$ can also be verified over the region $[0, 0.5] \times [1, 1.5] - [0, 0.15] \times [1, 1.1]$. The entire analysis is thus strongly correlated with the dynamical variation shown in Fig. 4c.

6 Conclusion

In this research, our main aim is to find the effect of noise in a nonlinear epidemic system and its complexity. To assure the impact of noise on the system, a stochastic sensitivity analysis is performed. The results indicate that noise strength is one of the major factors to enhance chaos in the system. Biologically it means a stable epidemic system can be more unpredictable at some extension of noise. The dynamical fluctuation was analyzed under the variation of K and R. It confirms chaotic dynamics can be observed in the system for a wide range of $(K,\ R)$. Finally, weighted entropy analysis is applied to investigate the complexity of both the noise free and noisy epidemic systems. It also assures a larger region of high complexity for the noise induced system than the same for the noise free system. As complex dynamics correspond to a destabilizing ecosystem,

our analysis confirms that the noisy epidemic system can be more unpredictable compared to the same in its deterministic part. In this way, we have established the effect of noise on the epidemic system.

Acknowledgements This work was supported by the Natural Science Foundation of China (Nos. 62061008, 61901530, 62071496), the Natural Science Foundation of Hunan Province (No. 2020JJ5767), the Science and Technology Foundation of Guizhou Province of China (No. [2018]1115), the Science and Technology Plan Project of Guizhou Province of China (No. [2018]5769), and the Doctoral Scientific Research Foundation of Guizhou Normal University (2017).

References

1. A. Hastings, C.L. Hom, S. Ellner, P. Turchin, H.C.J. Godfray, Annu. Rev Ecol. Systematics **24**, 1–33 (1993)
2. F. Takens, Lecture Notes Math. **898**, 366–381 (1981)
3. D.T. Kaplan, L. Glass, *Understanding Nonlinear Dynamics* (Springer, New York, 1995)
4. S. H. Strogatz, *Nonlinear Dynamics and Chaos* (Addison-Wesley, 1994)
5. E. Ott, *Chaos in Dynamical Systems* (Cambridge University Press, 1993)
6. L. Rondoni, M.R.K. Ariffin, R. Varatharajoo, S. Mukherjee, S.K. Palit, S. Banerjee, Opt. Commun. **387**, 257–266 (2017)
7. S. He, S. Banerjee, Physica A **501**, 408–417 (2018)
8. R.M. May, Nature **261**, 459–467 (1976)
9. A. Hastings, T. Powell, Ecology **72** (1991)
10. M.E. Gilpin, The. Am. Nat. **113**, 306–308 (1979)
11. Y. Takeuchi, N. Adachi, Bull. Math. Biol. **45**, 877–900 (1983)
12. A. Klebanoff, A. Hastings **122**, 221–233 (1994)
13. L. Gardini, R. Lupini, M. Messia, J. Math. Biol. **27**, 259–272 (1989)
14. K. Tanabe, T. Namba, Ecology **86**, 3411–3414 (2005)
15. A.-E.A. Elsadany, H. El-Metwally, E. Elabbasy, H. Agiza, Comput. Ecol. Softw. **2**, 169 (2012)
16. D.A. Rand, H.B. Wilson, Proc. R. Soc. B **246**, 179–184 (1991)
17. S. Higgs, Vector-Borne Zoonotic Dis. **6**, 115–116 (2006)
18. L. F. Olsen, G. L. Truty, W. M. Schaffer, Theor. population biology **33** (1988)
19. K. Das, S. Samanta, B. Biswas, J. Chattopadhyay, The. J. Ecol. **108**, 306–319 (2014)
20. F. Franchini, A.R. Its, V.E. Korepin, J Phys A **41**, 25302 (2008)
21. A. Kolmogorov, DoklAkad Nauk SSSR **124**, 754–5 (1959)
22. J.S. Richman, D.E. Lake, J.R. Moorman, Methin Enzymology **384**, 172–84 (2004)
23. S. He, S. Banerjee, Phys. A **490**, 366–77 (2018)
24. S. He, S. Banerjee, B. Yan, Complexity **2018**, 1–15 (2018)
25. B. Yan, S. Mukherjee, S. He, Eur. Phys. J. Spl. Top. **228**(12), 2769–77 (2019)
26. A. Eilersen, M.H. Jensen, K. Sneppen, Sci. Rep. **10**, 3907 (2020)
27. D. J. Earn, P. Rohani, B. T. Grenfell, Proc. Royal Soc. London. Ser. B: Biol. Sci. **265**, 7-10 (1998)
28. J.H. Brown, A. Kodric-Brown, Ecology **58**, 445–449 (1977)
29. B. Yan, S. Mukherjee, S. He, Eur. Phys. J. Spec. Top. **228**, 2769–2777 (2019)
30. S. Banerjee, M.R.K. Ariffin, Opt. Las. Tech. **45**, 435–442 (2013)
31. S. K. Palit, N.A.A. Fataf, M.R. Md Said, S. Mukherjee, S. Banerjee, Eur. Phys. J. Spec. Top. **226**, (2017) 2219-2234
32. T.S. Dang, S.K. Palit, S. Mukherjee, T.M. Hoang, S. Banerjee, Eur. Phys. J. Spec. Top. **225**, 159–170 (2016)
33. T.M. Hoang, S.K. Palit, S. Mukherjee, S. Banerjee, Optik **127**, 10930–10947 (2016)
34. G. A. Gottwald, I. Melbourne, Proc. R. Soc. Lond. A: Math., Phys. Engg. Sci. **460**, (2004) 603
35. G.A. Gottwald, I. Melbourne, Phys. Rev. E **77**, 028201 (2008)
36. C. Skokos, G.A. Gottwald, J. Laskar, Lecture Notes Phys. **915**, 221–247 (2016)
37. G.A. Gottwald, I. Melbourne, Phys. D **212**, 100–110 (2005)
38. Ya.. G. Sinai, Dokl. Russ. Acad. Sci. **124**, 768–771 (1959)
39. D. Daems, G. Nicolis, Phys. Rev. E **59**, 4000–4006 (1999)
40. A.N. Kolmogorov, I.R.E. Trans, Inf. Theory **2**, 102–108 (1956)
41. S. Mukherjee, S.K. Palit, S. Banerjee, M.R.K. Ariffin, L. Rondoni, D.K. Bhattacharya, Physica A **439**, 93–102 (2015)
42. S. Banerjee, S.K. Palit, S. Mukherjee, M.R.K. Ariffin, L. Rondoni, Chaos **26**, 033105 (2016)
43. S. Mukherjee, S. Banerjee, L. Rondoni, Physica A **508**, 131–140 (2018)
44. S. He, C. Li, K. Sun, S. Jafari, Entropy **20**, 556 (2018)
45. B. Yan, S.K. Palit, S. Mukherjee, S. Banerjee, Physica A **535**, 122433 (2019)
46. J.-P. Eckmann, S.O. Kamphorst, D. Ruelle, Europhys. Lett. **4**, 973–977 (1987)
47. N. Marwan, M. Carmen, Romano, M. Thiel, J. Kurths, Phys. Rep. **438**, (2007) 237-329
48. D. Eroglu, T. K. D. Peron, N. Marwan, F. A. Rodrigues, L. da F. Costa, M. Sebek, I.Z. Kiss, J. Kurths, Phys. Rev. E **90**, (2014) 042919
49. B. Fischer, Noise. J. Finance **41**, 529–543 (1986)
50. J.B. De Long, A. Shleifer, L.H. Summers, R.J. Waldmann, J. Political Econ. **98**, 703–738 (1990)
51. A. BenSaïda, Appl. Math. Comput. **226**, 258–265 (2014)
52. A. BenSaïda, Am. Int. J. Contemp. Res. **2**, 57–68 (2012)
53. I. Bashkirtseva, L. Ryashko, T. Ryazanova, Chaos. Solitons & Fractals **131**, 109549 (2019)

Springer Nature or its licensor holds exclusive rights to this article under a publishing agreement with the author(s) or other rightsholder(s); author self-archiving of the accepted manuscript version of this article is solely governed by the terms of such publishing agreement and applicable law.